Design and results of a first generation pilot plant for supercritical water desalination (SCWD)

Surika van Wyk[a,b,*], Samuel O. Odu[a,b], Aloijsius G.J. van der Ham[a], Sascha R.A. Kersten[a]

[a] Sustainable Process Technology, Faculty of Science and Technology, University of Twente, Postbus 217, 7500 AE Enschede, The Netherlands
[b] Wetsus, European Center of Excellence for Sustainable Water Technology, Oostergoweg, 98911 MA Leeuwarden, The Netherlands

ABSTRACT

A pilot plant of 5 kg/h based on the principle of supercritical water desalination (SCWD) has been designed, built and operated. The detailed design, operating procedures and performance of the plant is presented in this paper, along with the first results. Firstly, the plant has been tested for feed streams of 3.5 wt% NaCl to evaluate the stability and repeatability of the system, with the results indicating that mass balance closure is good and that reproducible results can be obtained. Furthermore, the results showed that 93% of the feed is recovered as fresh drinking water, which corresponds with expected results from phase equilibria simulations. The plant was further tested for higher feed concentrations of up to 16 wt% NaCl. For all feed concentrations, the NaCl concentration of the SCW was that of drinking water quality (< 600 ppm). Experimentally, using a single stage separator, a concentrated brine (38 wt% NaCl) was obtained and calculations showed that with a two-stage flash-evaporation scheme, zero liquid discharge (ZLD) can be obtained. Further modifications to the plant and tests with other salt mixtures are recommended in order to advance to industrial application.

1. Introduction

The demand for freshwater has risen in recent years due to the global population and industrialisation. The result is that many regions face a shortage of fresh drinking water and are not able to meet the current/growing demand from the existing freshwater resources [1,2]. For this reason, desalination technologies have been developed to convert saltwater to freshwater. In the past 20 years the global desalination capacity has increased with 58 million m³/d, with the capacity being 86.6 million m³/d in 2015 [3,4]. Desalination technologies are not only limited to seawater purification, but are also used to treat brackish water, river water, wastewater and brine. The purified water is used in numerous sectors including various industrial applications, power stations and tourism with municipal applications being the majority user. Conventional desalination technologies include reverse osmosis (RO), multi-stage flash distillation (MSF), multiple-effect evaporation (MEE) and electrodialysis (ED), with RO and MSF being the most used technologies [2]. Even though these technologies are well established, there are certain drawbacks such as low water recovery, ± 45% for seawater RO (SWRO) [5,6] and ± 50% for thermal processes such as MSF and MEE [6–9]. Parallel to the production of freshwater, these processes also generate brackish waste streams, which need to be managed. One of the major problems with the treatment of

the brine is the disposal into the oceans by coastal plants, which disrupts the ecosystems and threatens marine life. For plants located inland the brine streams are first treated before being discharged into bodies of water [1,2,10–12]. In recent years more stringent regulations have been put into effect for discharging the brines and for this reason zero liquid discharge (ZLD) technologies have been investigated and further developed [13,14]. ZLD technologies provide a manner to eliminate the production of brine streams, thereby reducing the impact of desalination on the environment. Supercritical water desalination (SCWD) is a technology, that presents a novel method of separating inorganic compounds from brackish water, with the potential of being ZLD technology [15,16].

At supercritical conditions (Pressure > 22.5 MPa, Temperature > 374 °C) the properties of water start to change significantly. The density of water decreases, which reduces the strength of the hydrogen bonds, causing the water to become non-polar. Consequently, the solubility of inorganic compounds reduces, which results in the formation of solid salt in supercritical water [16–18]. The removal of different inorganic salts from supercritical water has been extensively investigated in previous studies with various laboratory scale set-ups [19–26]. In our previous work [15], the potential of SCWD was investigated and presented. The phase equilibria of a NaCl-H₂O solution were measured on a laboratory scale set-up and the results
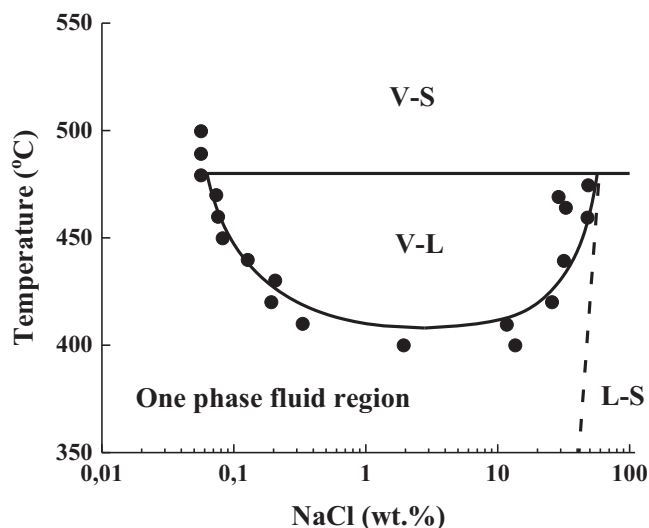

Fig. 1. Phase diagram of NaCl-H₂O system at 300 bar (- Anderko & Pitzer model [28]; – liquid–solid line [29]; ● experimental data [15]).

were used to illustrate the proof-of-principle of a two-stage separation process for SCWD. The first stage of separation is the continuous removal of supercritical water (SCW) from a liquid brine solution and occurs in the vapour–liquid (V–L) region at supercritical conditions (see Fig. 1). The next stage is the batch-wise separation of the liquid brine into salt and steam at subcritical conditions (100 °C and 1 bar). Additionally, heat integration, material selection and the controlled removal of salts at supercritical conditions was discussed. In a separate paper [27], the heat transfer mechanism of SCW flow at the mass fluxes and conditions expected in the SCWD pilot plant was investigated and used to design a heat exchanger for the pilot scale SCWD unit.

Recently, Ogden & Trembly [30] published results of a prototype Joule-heating desalination system (feed rate 6.1–6.7 kg/h brine), in which they experimentally investigated the thermodynamic properties of multicomponent brines at operating temperatures of 387 to 406 °C and pressures of 230 to 280 bar. In their paper, they present a plant based on Joule-heating, in which the brine is directly heated within the reactor, instead of externally as with the pilot plant introduced in the present paper. Also, the liquid brine is used to heat the feed to the unit, instead of the SCW.

Based on the experimental data and findings of our previous two papers [15,27] a first generation SCWD pilot plant was designed and built. In this paper, the design and layout of the plant will be presented and the performance will be evaluated. First experimental results for a feed of ± 3.5 wt% NaCl will be presented. Furthermore, the findings for higher saline feed (7–16 wt%) experiments will be given and discussed. The aim is to show the viability of the first generation SCWD process for the desalination of brackish water and its applicability for different concentration brine streams encountered in convectional desalination processes.

2. Pilot plant layout and key units

The pilot plant was designed and built at the high pressure laboratory of the University of Twente. The unit is located inside a concrete safety bunker and is fully automated so that it can be controlled from the outside during operation. The pilot plant has a maximum capacity of 8 kg/h of feed and was designed to operate at a maximum pressure of 380 bar and maximum temperature of 500 °C. The layout of the pilot plant is shown in Fig. 2.

From Fig. 2, it is seen that the pilot plant consists of several units, which can be divided into three sections namely the heat exchanger (HEX), gravity separator and brine recovery units (salt collector to

condensed vapour collector) (Sections 2.1 to 2.3). In addition to these units, there are two feed vessels and two product vessels. The first vessel contains demineralised water fed during the start-up and shut down of the system, while the other contains the saline feed. The first product vessel is for the collection of the drinking water coming from the gravity separator, while the second vessel is for the collection of the vapours produced during brine expansion. All vessels are placed on weighing balances to monitor the in- and out flow of the unit and to check the mass balance closure. A high-pressure LEWA diaphragm pump LDC1 (LEWA Herbert Ott GmbH & Co KG, Germany) is used to pressurise the saline feed. The pump has a maximum capacity of 25.0 L/h (with an uncertainty of 1% in mass flow measurements), a maximum operating pressure of 400 bar and is applicable to a wide variety of fluids including saline solutions. The feed pressure is set and controlled with a back pressure regulator, BPR-1 (TESCOM 26-1762-24A, Tescom Europe GmbH & Co. KG, Germany, $C_v = 0.14$).

2.1. Heat exchanger

Owing to the extreme operating conditions of SCW, the process is energy intensive and heat integration is required to make it commercially viable. For this unit, heat integration is achieved by utilising the SCW product to heat the saline feed in a heat exchanger that can operate from sub- to supercritical conditions. The feed will change from sub – to supercritical conditions, while the SCW will transition from super – to subcritical conditions. Prior to the design and construction of the heat exchanger, heat transfer characteristics of SCW was investigated through modelling in COMSOL Multiphysics and validated with experimental results [27].

From the findings, a double pipe counter-current heat exchanger was designed and constructed. The enthalpies for the design were determined from the correlations of Driesner [33] for the cold streams and the IAPWS formulation for the hot streams [49]. The inner and outer tubes of the heat exchanger are constructed from grade 2 titanium, with the dimensions listed in Table 1 (see Supporting information for detailed calculations). The double pipe heat exchanger is wound into a spiral coil (diameter of 40 cm and height of 40 cm) for stability and compactness. In the event of fouling due to salt deposition, the configuration of the heat exchanger is such that the saline feed is fed through the tube side, while the SCW product flows through the annular space (shell side) between the inner and outer tubes in a counter-current manner. Salt deposition from the feed can be easily cleaned, by running demineralised water through the system. To avoid contact between the inner surface and outer tube, a 0.5 mm titanium wire is wound around the outside of the inner tube before inserting it into the outer tube. The heat exchanger is also insulated with 20 mm thick glass fibre thermal insulation rope to reduce heat loss to the environment. In Fig. 3 the wound heat exchanger and inner tube with the 0.5 mm titanium wire is shown.

2.2. Gravity separator

In order to reach the desired feed temperature, additional heat is provided by an electrical heater located before the inlet to the gravity separator. The heater is comprised of a grade 2 titanium feed tube wound around a 2.5 kW aluminium block that provides the electrical heating.

The first stage of separation takes place in the gravity separator, where the SCW fluid phase is continuously separated from the concentrated liquid brine. The separator itself is constructed from Incoloy 825 with an inner diameter of 4 cm (wall thickness, $t = 2$ cm) and a length of 50 cm. The separator is placed in a 6 kW electric oven to ensure that isothermal conditions are maintained within the separator. The saline feed enters the separator though a dip-tube ($d_i = 3$ mm, $d_o = 5$ mm, $L = 20$ cm, grade 2 titanium), while the SCW fluid exits through the top, to the heat exchanger and liquid brine accumulates at
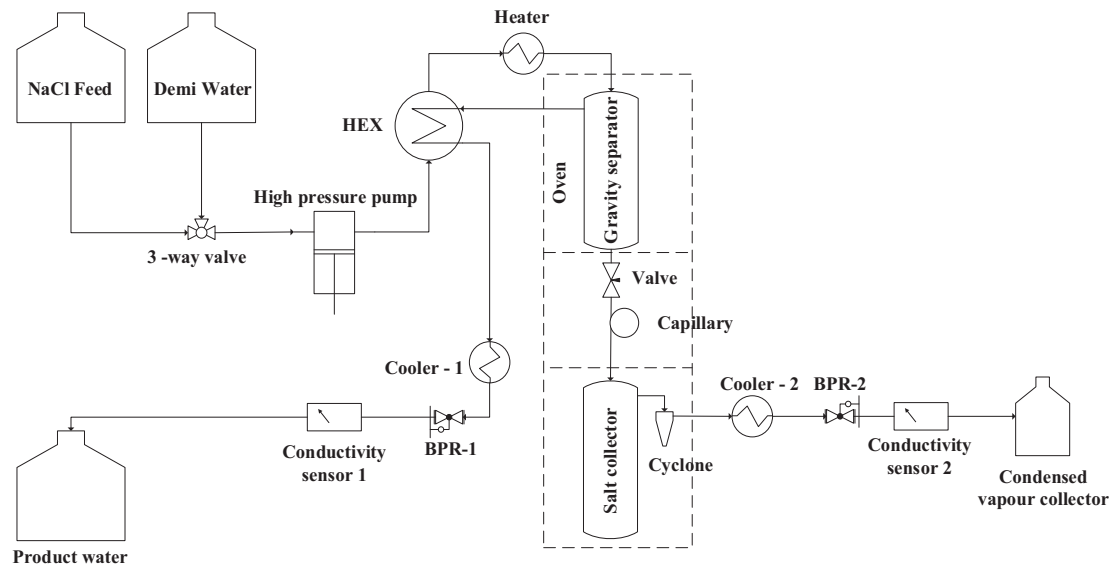
Fig. 2. SCWD pilot plant layout.

Table 1
Dimensions and material of bottom recovery unit.

Unit	Description	Dimensions	Material	Volume (L)
HEX	Double pipe heat exchanger, spiral shape. $A_o = 0.079 \, m^2$	$d_i = 3.0 \, mm$ $d_o = 5.0 \, mm$ $L = 5.0 \, m$	Inner tube – titanium	0.035
	Volume of annulus	$d_i = 6.2 \, mm$ $d_o = 9.5 \, mm$ $L = 5.0 \, m$	Outer tube – titanium	0.054
Separator	Gravity separator	$d_i = 40 \, mm$ $d_o = 80 \, mm$ $L = 50 \, cm$	Incoloy 825	0.628
Heater	Block heater for feed stream. Tube is spiral in Al block. $A_o = 0.071 \, m^2$	$d_i = 3.0 \, mm$ $d_o = 5.0 \, mm$ $L = 4.5 \, m$	Tube – titanium	0.032
Cooler-1	Water cooler $A_o = 0.028 \, m^2$	$d_i = 4 \, mm$ $d_o = 6 \, mm$ $L = 1.5 \, m$	Inner tube – SS 316	0.019
	Volume of annulus	$d_i = 8.0 \, mm$ $d_o = 10.0 \, mm$ $L = 1.5 \, m$	Outer tube – copper	0.033
Capillary	To flash brine into salt collector	$d_i = 7.0 \, mm$ $d_o = 10.0 \, mm$ $L = 32.0 \, cm$	Incoloy 825	0.012
Salt collector	Salt storage vessel	$d_i = 40 \, mm$ $d_o = 80 \, mm$ $L = 50 \, cm$	Incoloy 825	0.628
Cyclone	Separation of solid salt particles from water vapour	$d_i = 20 \, mm$ $d_o = 40 \, mm$ $L = 132 \, mm$	Incoloy 825	0.022
Cyclone collector	Collection of separated salt particles from cyclone	$d_i = 23.7 \, mm$ $d_o = 32.9 \, mm$ $L = 119.0 \, mm$	Incoloy 825	0.052
$3 \times$ Cooler-2	Water cooler $A_o = 0.11 \, m^2$	$d_i = 4 \, mm$ $d_o = 6 \, mm$ $L = 6.0 \, m$	Inner tube – SS 316	0.226
	Volume of annulus	$d_i = 8.0 \, mm$ $d_o = 10.0 \, mm$ $L = 6.0 \, m$	Outer tube – copper	0.396

the bottom of the separator.

After passing through the heat exchanger, the SCW is cooled to below the temperature limit of the back pressure regulator (70 °C) in water Cooler-1, after which it is depressurised and collected in the product water vessel. The dimensions of the discussed units are

summarised in Table 1.

2.3. Brine expansion and brine recovery units

The brine recovery section spans from the valve to the condensed vapour collector. For the second stage of separation, which is the expansion of the accumulated liquid brine, the high pressure – high temperature valve at the bottom of the gravity separator is fully opened to rapidly flash separate the brine into vapours and salt. The valve is made from a chromium-nickel based alloy creep resisting austenitic steel. It has a high resistance to corrosion and both stable mechanical and thermal properties at considerable high temperatures and pressures (up to 600 °C and 1000 bar). It is, therefore, suitable to handle the potentially corrosive brine and significant instantaneous pressure drop (up to 299 bar) during expansion of the brine. The valve is fully opened/closed pneumatically from the outside of the high-pressure bunker, using compressed nitrogen. Around both the valve and the capillary, a 1 kW oven is placed to ensure that the expansion of the brine occurs isothermally and to prevent premature formation of solid salt which could result in plugging.

The brine then expands inside the salt collector, which has the same dimensions as the gravity separator. In the cyclone, which follows the salt collector, the entrained salt particles are separated from the vapours into a secondary collector. Both are made from Incoloy 825. The design of the cyclone follows the methodology of Stairmand as stated in Sinnott [50]. Originally, the brine was directly expanded into the cyclone with the separated salt collected in the salt collector. However, a considerable amount of salt particles were entrained by the vapours resulting in high salt concentrations of the flashed vapours. It was, therefore, decided to change the sequence to where the brine is directly expanded into the salt collector. The vapours formed during the expansion in the salt collector, then moves to the cyclone for further separation of the entrained salt particles. The salt collector, cyclone and cyclone collector are placed inside a 6 kW oven with ceramic insulation to reduce heat loss to the environment and also to prevent the premature condensation of the formed vapours. The temperature of the oven is set to 100 °C, however some heat is transferred from the 1 kW oven causing the temperature of the top section of the salt collector to rise above 100 °C. This may skew the vapour recovery results to a limited extent. The expansion occurs within the 45 s and only the mass increase of that time interval is taken as the amount of vapours produced. Any mass increase recorded afterwards is taken as vapourisation
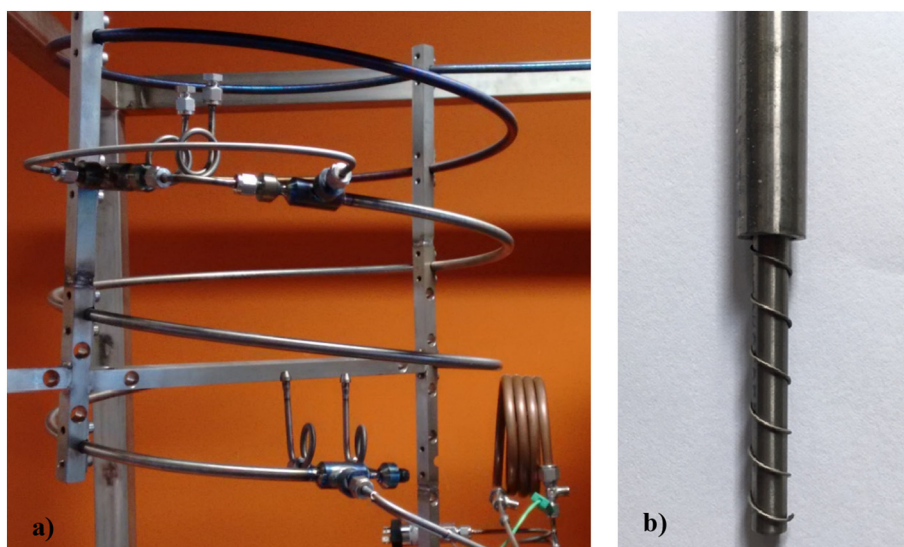
Fig. 3. Pictures of heat exchange section (a) spiral wound double pipe heat exchanger, (b) internal construction of the heat exchanger.

of the water in the salt collector. The vapours pass through three consecutive water coolers (Cooler-2) before being collected in the condensed vapour product vessel. The dimensions and material of construction of the above discussed units are summarised in Table 1.

Lastly, all temperature measurements are done with K-type thermocouples (uncertainty in temperature measurement is 0.4% of measured value in °C, while the relative difference of measured values between thermocouples is 0.2 °C), while the pressure measurements are done with sputtered thin film type pressure transducers (accuracy is 0.25% full scale).

3. Operation of pilot plant

3.1. Operating conditions

In order to validate the operation of the pilot plant, a set of five similar experiments were performed (referred to as the base experiments) to evaluate the repeatability and stability. For the base experiments, the feed concentration was 3.5 wt% NaCl, which corresponds to the feed salinity of seawater and is also the feed stream for SWRO and MSF [1,5,6,8]. The experimental uncertainties (within a 95% confidence level interval for the t-distribution) for the 3.5 wt% feed were determined, and these values were then also taken as the uncertainties for the higher feed concentration experiments. Experiments were performed for three higher feed concentrations, namely 7, 13.3 and 16 wt% NaCl. 7 wt% was selected to represent the retentate stream of a conventional RO unit and 16 wt% was selected to simulate a feed stream to an existing MEE plant for salt production [1,5,31].

The temperature and pressure for all the experiments were kept constant at 430 °C and 270 bar. 430 °C was selected as this was the maximum temperature in the V–L region where no premature salt deposition would occur at the outlet of the gravity separator. At higher temperatures, a shift to the L–S (see Fig. 1) region occurs upon the rapid decrease of pressure, causing salt deposition in the outlet of the separator. This hinders the collection of the bottom products and leads to plugging of the system. Preliminary experiments were also performed at higher temperature 440 and 450 °C with the results indicating that recovery of SCW was only 1% higher than for 430 °C, which further rationalised the use of this temperature.

For the operating pressure, the previous study by Odu et al. [15] stated that the plant should run at 300 bar, due to better operating stability and improved heat integration. For the pilot plant the pressure was set to 270 bar, as this is the maximum pressure that the plant could

operate at without leakages occurring during operation. At 300 bar, a difference (> 20%) in the mass balance was seen after some time of operation, while for 270 bar the mass balance differences was < 10% for the entire duration of the experiment. Analysis showed that leakages occurred due to the failure of a specific connection at 300 bar. With the current materials the connection could not be improved.

The feed rate and run time for the saline feed varied for the different concentrations due to faster accumulation of brine for more concentrated feed streams. The feed concentrations, flow rates and run times are summarised in Table 2.

3.2. Operating procedure

Prior to operation all fittings and connections were checked to ensure proper closure. The ovens of the gravity separator, flash valve with capillary section and salt collector were also switched on, so that the system is already heated before pressure is increased. The pilot plant is operated in a semi-batch mode, with the drinking water production being continuous and the salt recovery batch-wise. For the start-up, demineralised water is run through the system while pressure is gradually increased by adjusting the back-pressure regulator (BPR-1). The heater before the gravity separator is also switched on, to heat the feed to the desired separation temperature before entering the gravity separator. A mass balance is performed throughout, to ensure that the system is closed. Once the desired temperatures and pressures have been reached, the system is allowed to stabilise at the set conditions (maximum fluctuation of 1 °C and 2 bar for all measured temperatures and pressures for a 30 minute period).

After stabilisation, the saline feed is introduced to the system, by switching the three-way valve. The saline feed is prepared using demineralised water (resistivity of 15 MΩ·cm) and pharmaceutical grade NaCl (> 99.0%; esco API NaCl sodium chloride GMP grade) from esco. The pressured saline feed is heated in the counter-current heat exchanger, by the SCW product, with the remaining heat being supplied

Table 2
Feed flow rate and run time for different saline feed concentrations.

Feed concentration (wt% NaCl)	Feed rate (kg/h)	Run time (min)
3.0	5.3	64
7.0	5.5	23
13.3	2.2	33
16.0	1.0	47

by the heater before entering the gravity separator. Inside the separator phase separation occurs, based on a density difference, with the SCW fluid being continuously removed at the top, while the concentrated brine accumulates at the bottom. After passing through the heat exchanger the SCW is further cooled (Cooler-1) before being depressurised and analysed in line with a conductivity sensor (conductivity sensor 1, Fig. 2). The conductivity sensor was calibrated for a concentration range of 10^{-6} to 10 wt% NaCl, which was repeated multiple times throughout the experimental period. Linear behaviour was observed for the measured range of 0.05 to 0.07 wt%.

The plant is run with saline feed until the gravity separator is halfway filled with concentrated brine. Depending on the feed concentration and flow rate, the time of the operation varies from 20 to 60 min (see Table 2). The run time is predetermined for the different feed concentrations using the solubility data obtained from Driesner & Heinrich [32] and performing mass balance calculations.

Once the separator is halfway filled with brine, the feed is stopped and the valve between the gravity separator and salt collector is opened to rapidly flash separate the brine to 1 bar inside the salt collector. From the salt collector, the vapours and entrained salt particles flow to the cyclone, which separates the entrained salt particles and vapours. The vapours are then condensed, analysed inline (conductivity sensor 2, Fig. 2) and collected in the condensed vapour collector. The valve remains open until the pressure of the separator has stabilised at 1 bar. After stabilisation, the valve is closed and demineralised water is once more fed through the system to rinse it, while pressure is gradually decreased and the system is cooled.

Once ambient conditions are reached the salt collector and cyclone of the plant are removed and the products are retrieved for further analysis and mass balance calculations. The products retrieved consists of solid salt in both the salt and cyclone collector, some liquid water and condensed vapours. Dry salt is not obtained due to the enthalpy of the brine being insufficient for complete separation into dry salt and steam. Based on calculations made from the correlations of Driesner [32,33] the temperature and pressure would need to be 590 °C and 380 bar respectively, which is beyond the safe operating limits of the set-up. A one-stage flash will thus not result in a dry salt and steam stream. Calculations show that by expanding the brine in a normal flash, followed by flash-evaporation (using the produced steam of the first expansion) it is possible to completely separate the brine into dry solid salt and water (see Supporting information for calculations).

All temperatures and pressures are continuously recorded with PicoLog data acquisition. The mass of the demineralised water feed, saline feed, SCW product condensed vessel and vapour collector is also continuously monitored, using KERN BalanceConnection and is used to ascertain the mass balance closure during operation of the plant.

3.3. Analysis

The dissolved NaCl concentrations of the water retrieved from the bottom section of the pilot plant was determined by measuring the Na^+ concentration using ion chromatography (Metrosep C6 - 150/4.0 column on a Metrohm 850 Professional IC, mobile phase: 1.7 mM HNO_3 + 1.7 mM dipicolinic acid solution, column temperature: 20 ± 1 °C, flow rate: 1.0 mL/min). The moisture content was determined by drying the wet salt at 105 °C for 24 h and weighing the sample before and after.

3.4. Performance

3.4.1. SCW separation

An experimental run starts once saline feed is introduced into the system. Depending on the feed concentration and run time, the value of the NaCl concentration of the condensed supercritical water is registered every 5 to 15 min (continuously monitored), while the flow is continuously recorded. In Fig. 4a) & b) the flow rates of the feed and the

SCW is shown and also the NaCl concentration of the SCW product.

From Fig. 4a), it can be seen that the flow is stable within 5–15 min of operation. The NaCl concentration of SCW for the 7 wt% feed is lower than for the 3.5 wt% feed (see Fig. 4b). This is unusual as equal SCW concentrations are expected, since the feed concentration should not influence the equilibrium NaCl concentration of both products (SCW & brine). This could be the result of higher vapour flow rates for lower feed concentrations, causing more salt to be entrained. The SCW NaCl concentration for feeds of 3.5 and 7 wt% appear to stabilise within the first 15 min of operation. However, for higher feed concentrations the NaCl concentration seems to continue increasing with time, not stabilising before expansion of the brine. This could indicate that it takes longer for phase equilibrium to be reached for higher feed concentrations.

3.4.2. Brine expansion

In order to retrieve the accumulated brine in the gravity separator, it is expanded to 1 bar by opening the high temperature - high pressure valve. The expansion occurs rapidly being, completed within ± 1 min. In Fig. 5a) & b), the pressure and temperature change during expansion is shown.

From the figures, it is seen that the pressure and temperature inside the separator is stable for the duration of the run until the valve is opened. The pressure rapidly drops to 1 bar, where it stabilises while the valve remains open. Conversely, the pressure of the cyclone increases upon flashing of the brine. The temperature of the separator, capillary and valve also decreases with expansion of the brine. For the gravity separator, this is due to the flash evaporation of part of the water of the hot brine leaving the vessel as a consequence of the sudden drop in pressure. The capillary and valve are set to the same temperature (± 2 °C difference) as the separator and therefore the temperature will decrease due to the evaporation of water as a consequence of the pressure drop.

Premature salt deposition either before, after or inside the valve was the main challenge with the retrieval of the brine. During plugging the pressure drop was not as rapid as can be seen in Fig. 6a) & b).

In Fig. 6a) plugging before the valve is depicted with the consequence being that no bottom products are retrieved due to the brine remaining in the gravity separator. This type of plugging is caused by too high separation temperature. Upon rapid expansion the brine will move into the liquid solid (L–S) region (see Fig. 1), with the solid salt plugging the connection. At lower separation temperatures, the brine will remain liquid in the separator, before flashing over the valve and capillary, and finally separating into the solid salt, vapours and water. In Fig. 6b) plugging inside the capillary and valve is shown. It can be seen that the initial pressure drop is rapid but that it becomes more gradual with time. Consequently, some products are retrieved, but most remain in the gravity separator. The main cause of this type of plugging is owing to the construction of the capillary. Initially, it was too long and expansion did not occur adiabatically. As a result, the expansion was no longer isenthalpic and salt started to form inside the capillary and moved towards the valve, ultimately plugging the system. The inside diameter of the capillary was not uniform as a result of previous reparations, which also contributed to the plugging. It is foreseen that on industrial scale such severe plugging will occur less. Furthermore, upon salt deposition in the pipes, the system could be periodically flushed with water to remove the salt.

3.4.3. Corrosion

Corrosion has been identified as a key obstacle to the commercial success of SCW processes such as supercritical water oxidation (SCWO) and supercritical water gasification (SCWG) [34–36]. The high temperature and pressure conditions inherent to the SCWD process combined with the presence of salt could result in corrosion problems in the SCWD process. Due to its good mechanical and stable thermal properties over a wide temperature range as well as its exceptional resistance
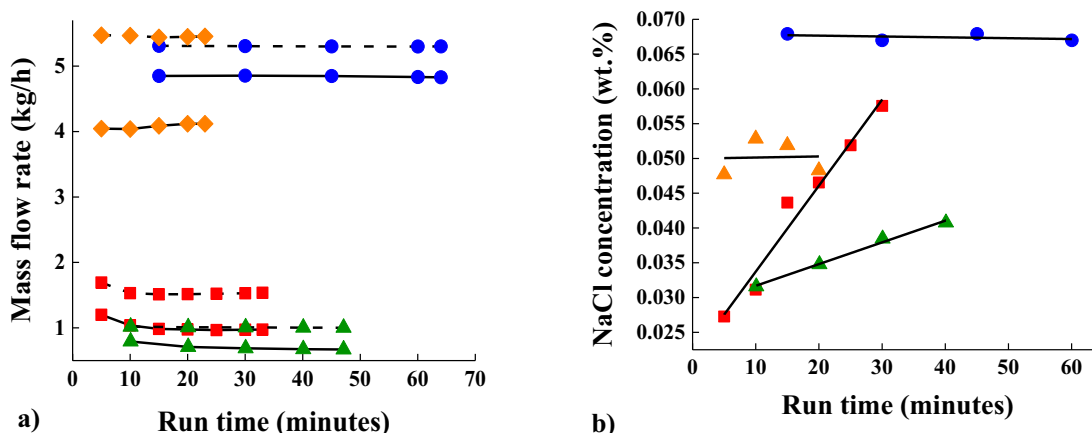
Fig. 4. Mass flow rates (a) and NaCl concentration of SCW (b) for different NaCl feeds (– feed stream; - SCW stream; ● 3.5 wt%; ◆ 7.0 wt%; ■ 13.3 wt%; ▲ 16.0 wt%).
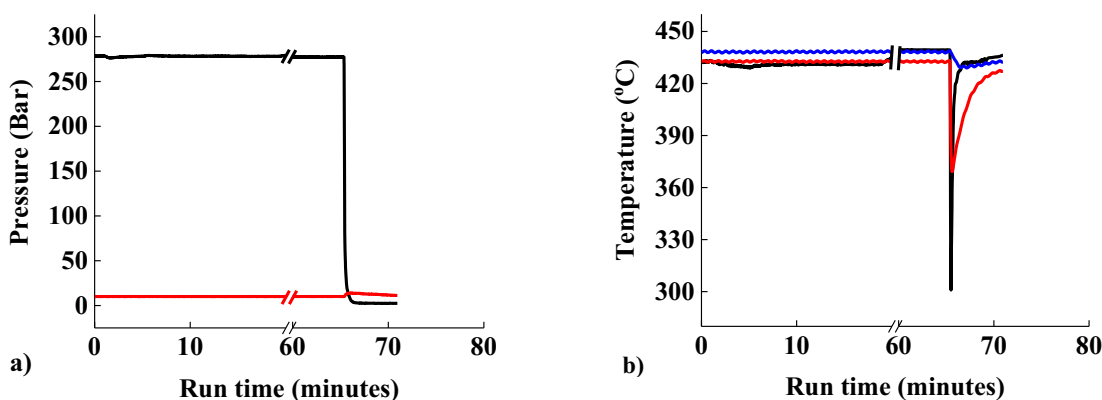

Fig. 5. Pressure (a) and temperature (b) change during brine expansion for 3.5 wt% NaCl feed ((a) ● gravity separator; ● cyclone; (b) ● gravity separator; ● capillary; ● valve).

to corrosion, Incoloy 825 (a nickel-iron-chromium alloy with additions of molybdenum, manganese, copper, and titanium) was chosen as the material of construction for the gravity separator, cyclone, cyclone collector and salt collector respectively. Considering cost and material properties such as the corrosion resistance and mechanical strength, grade 2 titanium has been chosen as the material of construction for the heat exchanger.

Despite the selection of the above materials, signs of corrosion were seen in the form of solids (not NaCl) in the condensed vapours samples, as well as in the water retrieved from the salt and cyclone collector. The solid deposition could be due to corrosion occurring in the reactor and the metals forming oxides when exposed to oxygen. Scatter electron

microscopy with energy dispersive spectroscopy (SEM – EDS; Jeol JSM 5600 LV, at 15 kV) was done on the solids separated from the water samples, to preliminarily determine the chemical elemental composition. The analysis indicated that the solids mainly contained iron and nickel. Other elements that could also be present are chromium, sodium and chloride. Copper and molybdenum were not detected. The presence of manganese was only detected for some samples. Lastly, there could also be trace amounts of titanium in some samples. From the analysis, it is concluded that the source of the metal oxides in the samples is mainly due to corrosion of Incoloy 825 and not the grade 2 titanium. A more detailed analysis is required to determine the exact composition of the metal oxides. In conclusion, it is seen that Incoloy 825 is not resistant
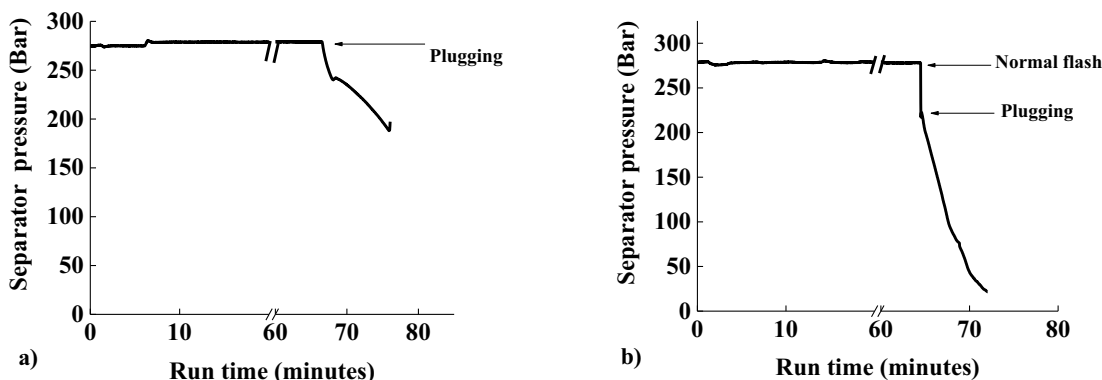

Fig. 6. Pressure drop of gravity separator during plugging.

Table 3
Summary of experimental conditions for base experiments and mass balance closure.

Exp.	NaCl feed (wt %)	Temperature (°C)	Pressure (bar)	Overall mass balance diff. (%)[a]	Salt mass balance diff. (%)[a]
1	3.0	430	272	1.0	3.8
2	3.0	431	271	1.1	−1.3
3	3.0	434	271	0.6	3.2
4	3.0	430	271	−0.2	4.8
5	3.6	431	273	0.6	−10.4

[a] Difference = ((Out − In) / In) ∗ 100.

enough to the extreme conditions and therefore the material of construction needs to be reconsidered. An option is to make use of a titanium lining inside the reactor.

4. Experimental results and discussion

In this section, the results of both the SCW production and brine expansion will be discussed. Firstly, the base experiment results will be presented, followed by the results for different feed concentrations.

4.1. Base experiments

The exact conditions for each experimental run as well as the mass balance closure for both the overall system and the salt are presented in Table 3.

The difference in the overall balance of the plant is < 2%, while that of the salt balance is slightly higher but still within acceptable limits for a pilot plant. The mass balance of the pilot plant is, therefore, considered to be closed. The products recovered from the SCWD unit is divided into two sections with the drinking water being retrieved from the gravity separator and solid salt, condensed vapours and some liquid water recovered from the bottom section, after expansion of the brine. In Table 4 the results of both the recovery (SCW/feed) and quality of drinking water and brine are given. The brine quality is reported on a calculated and measured basis. The calculated brine concentration is based upon mass balance calculations of the overall system and the NaCl, over the gravity separator using the conductivity readings of the SCW to calculate the NaCl concentrations. The measured brine concentration is based upon the retrieved products from the bottom section.

From the results, it is firstly seen that the recovery of drinking water and quality of both the brine and drinking water remained constant for the five experiments, indicating that reproducible data can be obtained. The average observed difference was < 6%, for the NaCl concentration the SCW and brine (within a 95% confidence level interval for the t-distribution). The recovery of drinkable water is ± 91 wt% of the feed and is significantly higher in comparison to conventional drinking water production processes such as MSF (15–50%) [6,9] and SWRO (30–50%) [1,37–39]. The NaCl concentration of the SCW (520 to 680 ppm) is below the maximum acceptable concentration level of total

Table 4
Product of the gravity separator both calculated and measured.

Exp.	SCW recovery (wt %)	SCW quality (NaCl wt%)	Brine quality – calculated (based on mass balance) (NaCl wt %)	Brine quality – measured (NaCl wt%)
1	91.6	0.065	34.7	32.4
2	91.4	0.058	33.9	29.7
3	91.1	0.052	32.4	31.4
4	90.6	0.059	31.6	33.7
5	91.4	0.068	39.8	33.3

Table 5
Comparison of experimental SCW NaCl concentrations at 430 °C and 270 bar of pilot plant with literature models.

	SCW quality (NaCl wt%)	Brine quality (NaCl wt%)
Experimentally measured (average of exp. 1–5)	0.06 ± 0.01	34.5 ± 3.2[a]
Armellini & Tester [19]	0.055	–
Anderko & Pitzer [28]	0.069	38.4
Driesner & Heinrich [32]	0.084	37.9

[a] Brine quality based on the average of the mass balance calculated concentrations.

dissolved solids (TDS) for clean drinking water by UNESCO, which is 750 ppm [40]. When comparing the results to the estimated values based on NaCl-H_2O equilibrium data, the expected SCW recovery for the given temperature and pressure is between 92 and 93 wt%, which is in good agreement with the results in Table 4. For the SCW NaCl concentration, the measured values were compared to the results of the empirical correlations by Driesner & Heinrich [32], the solvation model by Armellini & Tester [19] and the thermodynamic model by Anderko & Pitzer [28] (see Supporting information for detailed equations), as shown in Table 5.

From Table 5, it is seen that the experimental results and the model generated results compare well within one another and that the deviations are within the experimental uncertainty.

Comparison between the calculated and measured NaCl concentration of the brine shows that the latter is generally lower, with the maximum difference being 7 wt% (see Table 4). The difference can be ascribed to the loss of product when cleaning the bottom section of the plant as well as balance errors. It is, furthermore, assumed that all the brine is flashed to the bottom section with no salt remaining in the gravity separator. Under ambient conditions the maximum solubility of NaCl in water is 35.7 wt%, after which precipitation of solid salt occurs [41]. However, at supercritical conditions, a brine with concentrations up to 50 wt% (depending on the operating conditions) can be generated without solid deposition in the reactor. This concentrated brine could be a potential feed stream to processes where the feed concentration is limited to solubility of NaCl in water (see Section 5).

After expansion of the brine, the products (condensed vapour, salt and water) are distributed over four units in the bottom section, namely the salt collector, cyclone, cyclone collector and condensed vapour collector, with negligible amounts of product remaining in the pipes, valve and capillary. The qualitative distribution of the products is schematically shown in Fig. 7, for clarification on the product distribution results reported in Figs. 8 & 11.

In Fig. 7, it is indicated that wet solid salt is retrieved from both the salt - and cyclone collector, which forms the dry usable salt (after drying, see Section 3.3) retrieved from the pilot plant. NaCl concentrations of the water were generally between 15 and 25 wt%. For the condensed vapours the concentrations were between 10 and 18 wt%. The liquid water amount, in the salt and cyclone collector, is the summation of the water (excluding NaCl) and the moisture in the wet salt. The condensed vapours are the amount of water in the condensed vapour collector excluding the dissolved NaCl content. The product distribution of the flashed products is given in Fig. 8. The brine content was normalized to a value of 100% and the distribution in the bottom units were calculated as a fraction of the brine content.

For Fig. 8, the total water content of the brine is equal to the sum of the water content of the salt collector, cyclone, cyclone collector and the condensed vapour collector. Likewise, the total dissolved NaCl content of the brine is equal to the sum of the dissolved and solid NaCl content of the salt and cyclone collector, and the dissolved NaCl concentration of the cyclone and condensed vapour collector. From the product distribution results, it can be seen that most of the water in the
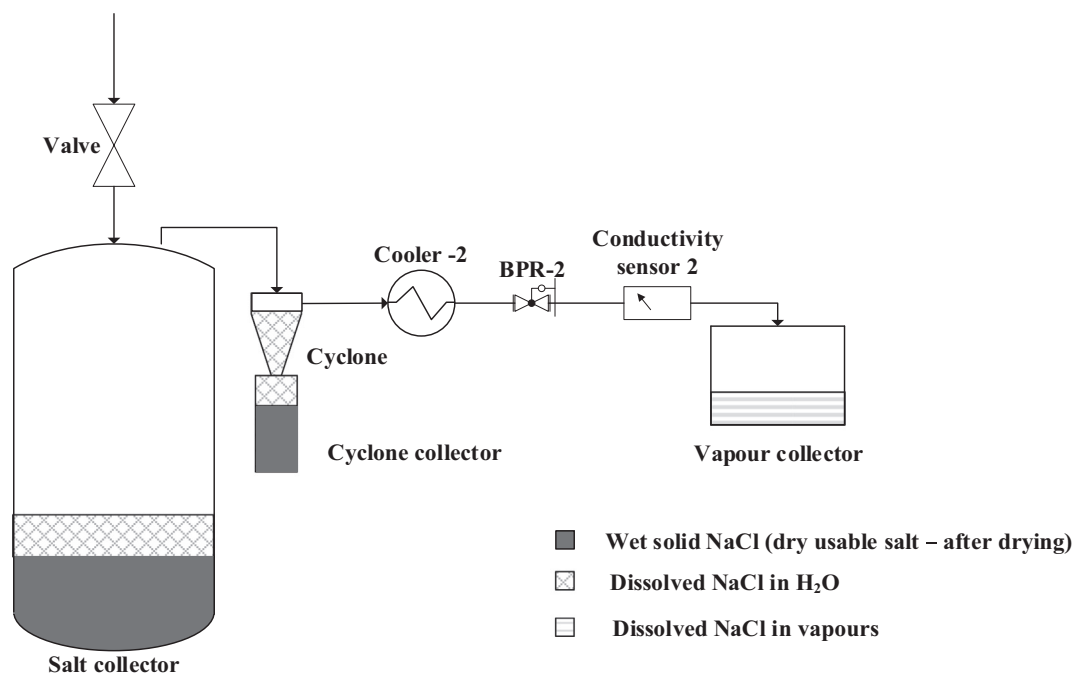
Fig. 7. Qualitative product distribution in bottom section of pilot plant (levels and sizes are not to scale).

brine forms condensed vapours, with ± 14% forming liquid water in the other collectors. Conversely, most of the dissolved NaCl in the brine, forms solid NaCl in the salt collector. Together with the solid salt in the cyclone collector, the total solid salt recovery (solid NaCl/NaCl fed to plant) is ± 64%, which corresponds to ± 175 g of salt. The main reason for loss of salt is due to entrainment of the fine salt particles upon flash separation. The separation occurs rapidly (< 1 min) leaving no time for crystallisation or agglomeration of the salt particles. The resulting particle size is between 2 and 15 μm (determined by SEM analysis) which is easily entrained with the vapours to the condensed vapour collector. The cyclone is also not effective in separating the salt from the vapours because of the small particle size. It is estimated, from the salt mass balance calculations over the bottom section of the pilot plant, that only 30–46% of the entrained solids are removed from the vapour stream.

From Fig. 8, it can be seen that the condensed vapour collector contains the highest amount of dissolved NaCl. The resulting NaCl concentration in the condensed vapour is usually between 10 and 18 wt %. The separation of the water vapour and salt should therefore be improved and is part of future research. Secondary to entrainment, some of the salt is also dissolved in the liquid water present in the salt and cyclone collector, but these amounts are minimal in comparison to

that of the condensed vapours and can be retrieved through evaporation of the water.

4.2. Different feed concentrations

In order to further test the applicability of the pilot plant with other desalination/salt production processes, feed streams with higher salinities were also investigated. For these experiments, the temperatures and pressures were kept similar to the base experiments, however, the feed rate and run time had to be adjusted to ensure that the gravity separator was only half-way filled with brine, before expansion. A summary of the experimental conditions is given in Table 6, along with the mass balance closures.

For the overall mass balance, the closure is within 8%, while for the salt balance the difference increases for higher feed concentrations. The exact cause is not clear but a possible reason could be that at higher feed concentrations some of the salt precipitates and adheres to the wall of the gravity separator. Consequently, the salt then remains in the gravity separator after expansion of the brine and is not retrieved. The SCW recovery as well as the SCW NaCl concentrations are reported in Figs. 9 & 10.

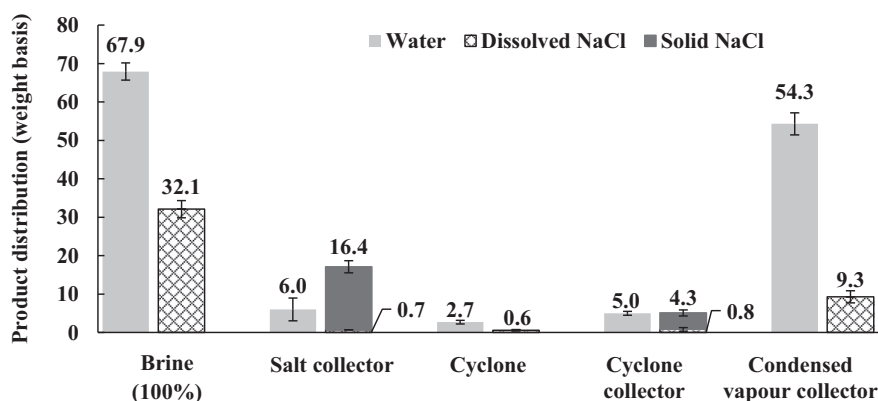For Fig. 10, for 13.3 and 16 wt% the average concentration over the

Fig. 8. Product distribution of normalized brine (values based on measured brine from collected bottom products) (Mass balance is: ■ brine = ■ salt collector + ■ cyclone + ■ cyclone collector + ■ condensed vapour collector; ⊠ brine = (⊠ + ■) salt collector + ⊠ cyclone + (⊠ + ■) cyclone collector + ⊠ condensed vapour collector).

Table 6
Summary of experimental conditions for different feed concentrations and mass balance closure.

NaCl feed (wt%)	Temperature (°C)	Pressure (bar)	Overall mass balance diff. (%)[a]	Salt mass balance diff. (%)[a]
3.0	431	272	0.6	2.6
7.0	429	271	−1.9	−8.2
13.3	432	272	1.5	−18.4
16.0	434	271	7.8	−16.9

[a] Difference = ((Out − In) / In) * 100.
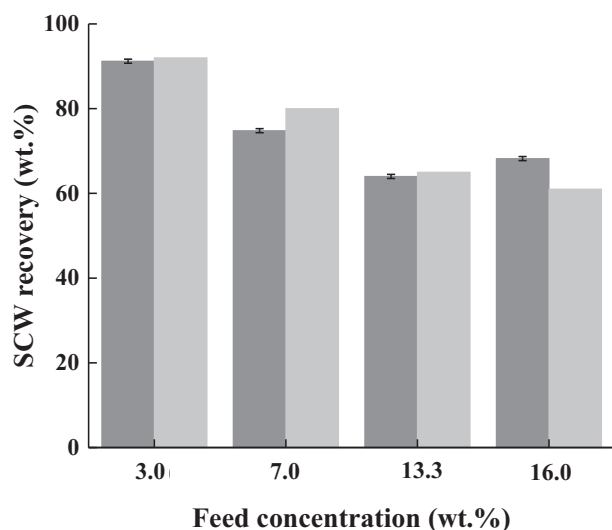
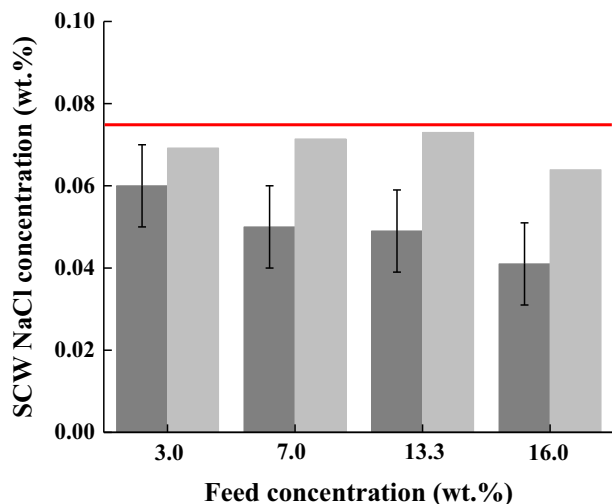**Fig. 9.** SCW recovery for different feed streams (■ experimental; ■ model [28,32]).

Fig. 10. SCW quality for different feed streams (■ experimental; ■ model [28]; ▬ safe drinking limit for water 750 ppm).

run time has been taken. From the results, it is seen that the recovery of SCW decreases with feed concentration (with the exception of 16 wt%) while, the NaCl concentration of the SCW also seems to decrease. The NaCl concentration of both the SCW should not vary for different feed concentrations since it is only dependent on the temperature and pressure of the system. Only the quantity of SCW should differ with feed concentration. This is seen when comparing the results of the model in Figs. 9 and 10 for the different feed concentrations. For the feed concentrations of 3.0 to 13.3 wt% the SCW recovery corresponds

adequately with what is expected from phase equilibria calculations [28,32], whereas the measured NaCl concentration of the SCW is once more lower in comparison to the results of the Anderko & Pitzer model [28]. For 16.0 wt%, the SCW recovery is higher (± 10%) than expected from NaCl-H₂O equilibria. This is most likely due to equilibrium not being reached within the system and for this reason the NaCl concentration of the SCW is also lower in comparison. Tests with higher feed concentrations were also performed on our laboratory-scale [15] set-up and the same SCW recovery was measured, as for the pilot plant. To resolve the problem of equilibrium not being reached, a larger vessel is required, since the pump's minimum flow limitations have already been reached. The overall product distribution, of the expanded brine, is presented in Fig. 11.

Upon comparison of the three figures and Fig. 8, it is seen that the water content of the salt collector increases, along with the amount of dissolved NaCl. The higher water content could also be due to equilibrium not being reached for higher feed concentrations.

As a consequence of the higher liquid water content the salt recovery decreases due to more salt being dissolved. The salt recovery decreased to 51% for a feed of 7 wt% and to 42–44% for the higher feed concentrations. For the base experiments, the main loss of salt was due to entrainment of salt particles with the vapours. However, for higher feed concentrations the solvation of salts in the liquid water also contributes significantly to the loss. When comparing the absolute values of dissolved salt, the amount increased from 15 g for a feed concentration of 3 wt% to 20–30 g for feed concentrations of 7 wt% and higher. Conversely, the absolute amount of entrained salt decreased from 51 g to 15–38 g for higher feed concentrations, while the total amount of salt remained constant.

4.3. Heat exchanger performance

The results of the heat exchanger performance for 3.0, 7.0 and 16.0 wt% are presented in Table 7.

It is observed, that the ΔT_{Shell} is higher than ΔT_{Tube} which is due to the difference in heat capacity and mass flow rates. The losses of the heat exchanger were calculated to be between 16 and 25%. In order to improve this, the sides can be switched or better quality insulation can be used. It is concluded that the heat exchanger is functioning properly for the given experiments.

5. Future outlook and industrial application

Before industrial application, further testing is required to refine the SCWD process. After the initial evaluation of the pilot plant performance and experimental results the following recommendations are made for improvement of the SCWD unit:

- Investigate the influence of other salts and salt mixtures, that are also present in conventional desalination feed streams *e.g.* Na₂SO₄ and K₂SO₄. Typically the feeds to desalination units are first pre-treated to remove salts such as Mg(OH)₂, CaCO₃ and SrCO₃, which could cause severe fouling [42]. The main drawback would be the presence of Na₂SO₄ and K₂SO₄, which form a solid-fluid equilibrium at supercritical conditions. The formation of solids would lead to the fouling and possible plugging of the separator. Studies have shown that for NaCl-Na₂SO₄-H₂O mixtures, vapour-liquid equilibrium can be reached for higher feed concentrations of NaCl, and therefore the problem of solid formation can be counteracted [43,44].
- An in-depth material of construction study is required to select a more corrosion resistant material. Another improvement can be made by constructing the reactor from stainless steel and then lining the inside with titanium to reduce corrosion, since only trace amounts of titanium were detected in the metal oxide samples.
- The design of the cyclone system needs to be improved so that it is able to more efficiently separate the fine salt and vapours, for better
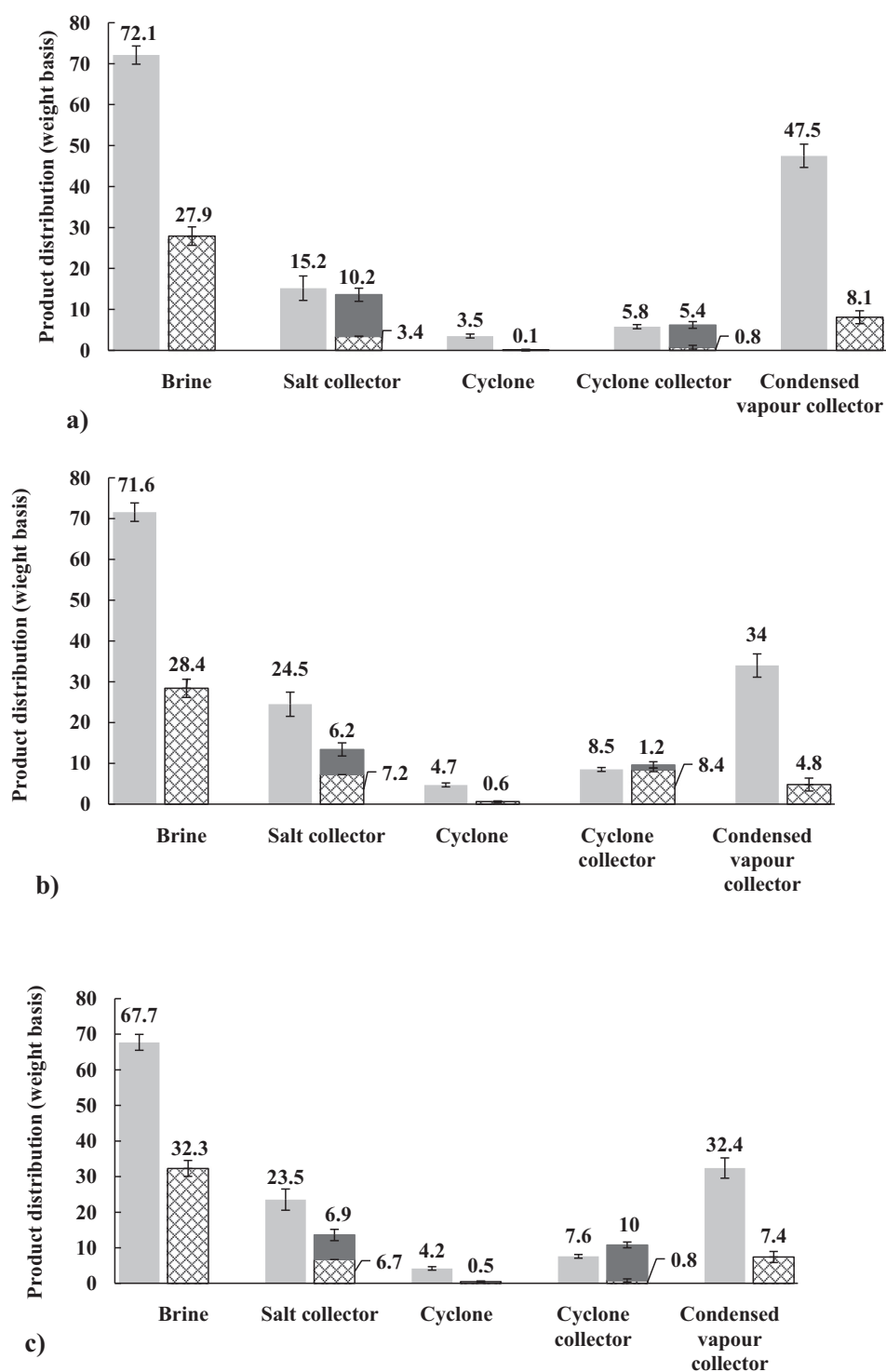
Fig. 11. Product distribution of normalized brine (values based on measured brine from collected bottom products) for different feed concentrations (a) 7.0 wt%, (b) 13.3 wt%, (c) 16.0 wt% (▨ water; ▨ dissolved NaCl; ■ solid NaCl).

Table 7
Heat exchanger performance for different feed concentrations at 270 ± 2 bar.

Feed (wt %)	Feed flow (kg/h)	SCW flow (kg/h)	Tube		Shell	
			T_{in} (°C)	T_{out} (°C)	T_{in} (°C)	T_{out} (°C)
3.0	5.3	4.8	17	370	404	31
7.0	5.5	4.1	28	328	346	32
16.0	1.0	0.7	26 (25.6)	313	313	27 (26.7)

quality vapours and higher salt recoveries. A possible improvement could be placing the cyclones in series.

- Adjustments should also be made so that the pilot plant can run longer for more concentrated feed solutions, so that steady state can be reached before brine expansion. This can be achieved by using a different pump with lower flow rates and/or by increasing the size of the gravity separator.

- At this stage only the heat is recovered from the SCW stream, however, this stream is also pressurised (270 bar) and actions should be taken to recover the pressure of the stream to partially pressurise the feed stream, similar to what is done for RO systems [45,46].

- Lastly, the recovery of the brine stream is at this stage a batch-wise process but could be altered that it becomes a continuous process, with the flashed vapours being recycled back to the feed and the salt recovered as a slurry. The configuration of the brine retrieval is, however, dependent on the process it will be integrated with. For a MEE salt production process the brine could be directly mixed with the feed stream.

For industrial application the SCWD plant, as a stand-alone unit, would be too energy intensive to compete with conventional desalination technologies. From previous work [15], it was estimated that the energy consumption of the unit would be 450 MJ$_{th}$/m^3 drinking water (after heat integration), which is much higher in comparison to conventional processes such as SWRO (30 MJ$_{el}$/m^3) and MSF (300 MJ$_{th}$/m^3) [8]. However, SCWD has a higher freshwater recovery, produces solid salt and could potentially be ZLD. Additionally, SCWD could also assist with the elimination of organic micro pollutants/pollutants in water. Vadillo et al. [47] stated that SCWO is a promising technology to treat a wide variety of wastewaters due to the high reaction rates and temperatures, which decreases the time required for destruction of the pollutants. SCWO, however, occurs in the presence of oxygen, while SCWD occurs in the absence of oxygen. Therefore, SCWD could be integrated with existing desalination processes as either a pre – or post treatment step, to improve the feed quality to the units or help manage the brine discharge of existing technologies.

A RO recovery unit usually produces a retentate waste stream with a concentration of 7 wt% NaCl at a pressure of 6–7 MPa [1,5,48]. For this case, the SCWD unit can serve as a post treatment step to treat the retentate waste stream, as the stream is already partially pressurised and the unit is able to separate feeds containing 7 wt% NaCl. The SCW stream could then be combined with the drinking water recovered from the RO unit. The heat of the SCW stream could also be used to heat the feed and pressurise either the RO feed stream or the SCWD feed stream through a heat exchanger and pressure exchanger respectively.

Another possible application is as a pre-treatment for MEE. The typical feed concentrations for MEE plants are between seawater to concentrated brines of 17–25 wt% [6,8,31]. At supercritical conditions brines with concentrations between 30 and 50 wt% are produced, without salt precipitation. The produced brine could be combined with the feed stream of an MEE unit to increase the NaCl feed concentration. Additionally, the heat from the brine could be used to heat the feed stream so that conventional steam is no longer required, which could reduce the overall energy consumption. These integrations will be studied in the future.

Recently, a conceptual design and economics study was done by Lopez & Trembly [42] to assess the preliminary economics of a standalone SCWD unit with chemical precipitation pre-treatment. Their findings showed that the SCWD unit was more costly in comparison to RO and other combined RO processes, however, SCWD has the potential to be ZLD technology and is able to treat more concentrated streams (hypersaline streams).

6. Summary and conclusions

A first generation SCWD pilot plant has been designed, constructed and tested for different saline feeds. Experiments were firstly performed for a feed concentration of 3.5 wt% NaCl, with the performance and stability of the unit being evaluated. The system was at steady state within 15 min of the saline feed being introduced. Expansion of the brine is a rapid process and no plugging occurred, after the correct conditions were established. Incoloy 825 showed signs of corrosion and a titanium lined system is proposed.

From the base experimental findings, it is concluded that the system's mass balance is closed and that reproducible data can be obtained. The recovery of fresh drinking water was higher in comparison to conventional processes and corresponded with expected phase equilibria results. The quality of SCW adhered to the requirements for drinking water having a NaCl concentration between 520 and 680 ppm (safe limit is < 750 ppm TDS). The bottom product distribution showed that mainly vapours are formed, followed by salt and liquid water. The recovery of salt was (solid NaCl/NaCl fed to plant) ± 64%, with the main loss being due to entrainment of the fine salt particles (2–15 μm) with the vapours. Calculations showed that ZLD is possible using a two-stage flash with heat integration.

For the different feed concentrations, the SCW recovery decreased and corresponded with phase equilibria results up to a feed concentration of 13.3 wt%, while for a feed of 16 wt% NaCl equilibrium is not reached and the SCW recovery is unexpectedly higher. For the bottom products, the total amount of salt remained constant, while the amount of vapours decreased and the liquid water increased. Consequently, the solid salt recovery decreased due to more salt being dissolved in the liquid water.

The temperature profiles of the heat exchanger were evaluated from which it was concluded that the heat exchanger is functioning properly.

Due to the energy intensive nature of the unit it is recommended that the SCWD unit be integrated with a conventional desalination process to treat the concentrated brine stream and obtain an overall ZLD process, but further study is still required to refine the process.

Nomenclature

BPR	back-pressure regulator
ED	electrodialysis
EDS	energy dispersive spectroscopy
HEX	heat exchanger
L–S	liquid–solid
MEE	multiple-effect evaporation
MSF	multi-stage flash
RO	reverse osmosis
SCW	supercritical water
SCWD	supercritical water desalination
SCWG	supercritical water gasification
SCWO	supercritical water oxidation
SEM	scatter electron microscopy
SWRO	seawater reverse osmosis
TDS	total dissolved solids
V–L	vapour–liquid
V–S	vapour–solid
ZLD	zero liquid discharge

Symbols

a	Helmholtz free energy
A_o	heat transfer area
A_2, A_3	second – and third order perturbation terms
$\dot{Q}$	heat flow
R	gas constant
T	temperature
u	velocity
U	overall heat transfer coefficient
v	volume
x	mole fraction

Greek symbols

Δ	difference
ρ	density
Φ	volume flow
η	reduced density
σ	hard-sphere diameter
μ	dipole momentum

Subscripts

c	cold
h	hot
ht	heater
l	liquid
lm	logarithmic mean
i	inner
o	outer
per	perturbation
ref	reference
rep	repulsive
res	residual
t	terminal
v	vapour
w	water

Appendix A. Supplementary data

Supplementary data to this article can be found online at https://doi.org/10.1016/j.desal.2018.03.028.

References

[1] V.G. Gude, Desalination and sustainability - an appraisal and current perspective, Water Res. 89 (2016) 87–106, http://dx.doi.org/10.1016/j.watres.2015.11.012.

[2] D. Xevgenos, K. Moustakas, D. Malamis, M. Loizidou, An overview on desalination & sustainability: renewable energy-driven desalination and brine management, Desalin. Water Treat. 3994 (2014) 1–11, http://dx.doi.org/10.1080/19443994.2014.984927.

[3] A. Bennett, 50th anniversary: desalination: 50 years of progress, Filtr. Sep. 50 (2013) 32–39, http://dx.doi.org/10.1016/S0015-1882(13)70128-9.

[4] IDA, Desalination by the Numbers, Int. Desalin. Assoc., 2017.

[5] L.F. Greenlee, D.F. Lawler, B.D. Freeman, B. Marrot, P. Moulin, Reverse osmosis desalination: water sources, technology, and today's challenges, Water Res. 43 (2009) 2317–2348, http://dx.doi.org/10.1016/j.watres.2009.03.010.

[6] V.G. Gude, Energy storage for desalination processes powered by renewable energy and waste heat sources, Appl. Energy 137 (2015) 877–898, http://dx.doi.org/10.1016/j.apenergy.2014.06.061.

[7] N. Ghaffour, T.M. Missimer, G.L. Amy, Technical review and evaluation of the economics of water desalination: current and future challenges for better water supply sustainability, Desalination 309 (2013) 197–207, http://dx.doi.org/10.1016/j.desal.2012.10.015.

[8] J.E. Miller, Review of water resources and desalination techniques, Sand Rep. (2003) 1–54 (doi:SAND 2003-0800).

[9] V. Fulya, MENA Regional Water Outlook: Part II Desalination Using Renewable Energy, Fichtner, 2011, p. 24 (doi:6543P07/FICHT-7109954-v2).

[10] I.S. Al-Mutaz, Features of multi-effect evaporation desalination plants, Desalin. Water Treat. 54 (2015) 3227–3235, http://dx.doi.org/10.1080/19443994.2014.910842.

[11] S. Lattemann, T. Höpner, Environmental impact and impact assessment of seawater desalination, Desalination 220 (2008) 1–15, http://dx.doi.org/10.1016/j.desal.2007.03.009.

[12] A. Giwa, V. Dufour, F. Al Marzooqi, M. Al Kaabi, S.W. Hasan, Brine management methods: recent innovations and current status, Desalination 407 (2017) 1–23, http://dx.doi.org/10.1016/j.desal.2016.12.008.

[13] D. Xevgenos, K. Moustakas, D. Malamis, M. Loizidou, An overview on desalination & sustainability: renewable energy-driven desalination and brine management, Desalin. Water Treat. 57 (2016) 2304–2314, http://dx.doi.org/10.1080/19443994.2014.984927.

[14] H.W. Chung, K.G. Nayar, J. Swaminathan, K.M. Chehayeb, J.H. Lienhard V, Thermodynamic analysis of brine management methods: zero-discharge desalination and salinity-gradient power production, Desalination 404 (2017) 291–303, http://dx.doi.org/10.1016/j.desal.2016.11.022.

[15] S.O. Odu, A.G.J. Van Der Ham, S. Metz, S.R.A. Kersten, Design of a process for supercritical water desalination with zero liquid discharge, Ind. Eng. Chem. Res. 54 (2015) 5527–5535, http://dx.doi.org/10.1021/acs.iecr.5b00826.

[16] S.J. Metz, I. Leusbrock, Method and system for supercritical removal of an inorganic compound, US 2011/0180384 A1, 2011.

[17] F.J. Armellini, J.W. Tester, Experimental methods for studying salt nucleation and growth from supercritical water, J. Supercrit. Fluids 4 (1991) 254–264, http://dx.doi.org/10.1016/0896-8446(91)90020-7.

[18] M. Hodes, P.A. Marrone, G.T. Hong, K.A. Smith, J.W. Tester, Salt precipitation and scale control in supercritical water oxidation - part a: fundamentals and research, J. Supercrit. Fluids 29 (2004) 265–288, http://dx.doi.org/10.1016/S0896-8446(03)00093-7.

[19] F.J. Armellini, J.W. Tester, Solubility of sodium chloride and sulfate in sub- and supercritical water vapor from 450–550 °C and 100–250 bar, Fluid Phase Equilib. 84 (1993) 123–142, http://dx.doi.org/10.1016/0378-3812(93)85120-B.

[20] I. Leusbrock, S.J. Metz, G. Rexwinkel, G.F. Versteeg, The solubilities of phosphate and sulfate salts in supercritical water, J. Supercrit. Fluids 54 (2010) 1–8, http://dx.doi.org/10.1016/j.supflu.2010.03.003.

[21] I. Leusbrock, S.J. Metz, G. Rexwinkel, G.F. Versteeg, Solubility of 1:1 alkali nitrates and chlorides in near-critical adn supercritical water, J. Chem. Eng. Data 54 (2009) 3215–3223.

[22] I. Leusbrock, S.J. Metz, G. Rexwinkel, G.F. Versteeg, The solubility of magnesium chloride and calcium chloride in near-critical and supercritical water, J. Supercrit. Fluids 53 (2010) 17–24, http://dx.doi.org/10.1016/j.supflu.2009.12.015.

[23] M. Schubert, J. Aubert, J.B. M??ller, F. Vogel, Continuous salt precipitation and separation from supercritical water. Part 3: interesting effects in processing type 2 salt mixtures, J. Supercrit. Fluids 61 (2012) 44–54, http://dx.doi.org/10.1016/j.supflu.2011.08.011.

[24] M. Schubert, J.W. Regler, F. Vogel, Continuous salt precipitation and separation from supercritical water. Part 2. Type 2 salts and mixtures of two salts, J. Supercrit. Fluids 52 (2010) 113–124, http://dx.doi.org/10.1016/j.supflu.2009.10.003.

[25] M. Schubert, J.W. Regler, F. Vogel, Continuous salt precipitation and separation from supercritical water. Part 1: type 1 salts, J. Supercrit. Fluids 52 (2010) 99–112, http://dx.doi.org/10.1016/j.supflu.2009.10.002.

[26] P. Dell'Orco, H. Eaton, T. Reynolds, S. Buelow, The solubility of 1: 1 nitrate electrolytes in supercritical water, J. Supercrit. Fluids 8 (1995) 217–227.

[27] S.O. Odu, P. Koster, A.G.J. Van Der Ham, M.A. Van Der Hoef, S.R.A. Kersten, Heat transfer to sub- and supercritical water flowing upward in a vertical tube at low mass fluxes: numerical analysis and experimental validation, Ind. Eng. Chem. Res. 55 (2016) 13120–13131, http://dx.doi.org/10.1021/acs.iecr.6b03268.

[28] A. Anderko, K.S. Pitzer, Equation-of-state representation of phase equilibria and volumetric properties of the system NaCl-H2O above 573 K, Geochim. Cosmochim. Acta 57 (1993) 1657–1680, http://dx.doi.org/10.1016/0016-7037(93)90105-6.

[29] L. Bischoff, K.S. Pitzer, Liquid-vapour relations for the system NaCl-H2O: summary of the P-T-x surface from 300° to 500 °C, Am. J. Sci. 289 (1989) 217–248.

[30] D.D. Ogden, J.P. Trembly, Desalination of hypersaline brines via Joule-heating: experimental investigations and comparison of results to existing models, Desalination 424 (2017) 149–158, http://dx.doi.org/10.1016/j.desal.2017.10.006.

[31] R. Kaplan, D. Mamrosh, H.H. Salih, S.A. Dastgheib, Assessment of desalination technologies for treatment of a highly saline brine from a potential CO2 storage site, Desalination 404 (2017) 87–101, http://dx.doi.org/10.1016/j.desal.2016.11.018.

[32] T. Driesner, C.A. Heinrich, The system H2O-NaCl. Part I: correlation formulae for phase relations in temperature-pressure-composition space from 0 to 1000 °C, 0 to 5000 bar, and 0 to 1 XNaCl, Geochim. Cosmochim. Acta 71 (2007) 4880–4901, http://dx.doi.org/10.1016/j.gca.2006.01.033.

[33] T. Driesner, The system H2O-NaCl. Part II: correlations for molar volume, enthalpy, and isobaric heat capacity from 0 to 1000 °C, 1 to 5000 bar, and 0 to 1 XNaCl, Geochim. Cosmochim. Acta 71 (2007) 4902–4919, http://dx.doi.org/10.1016/j.gca.2007.05.026.

[34] P.A. Marrone, G.T. Hong, Corrosion control methods in supercritical water oxidation and gasification processes, J. Supercrit. Fluids 51 (2009) 83–103, http://dx.doi.org/10.1016/j.supflu.2009.08.001.

[35] D.M. Harradine, P.C. Buelow, P.C. Dell'Orco, R.B. Dyer, B.R. Foy, J.M. Robinson, J.A. Sanchez, T. Spontarelli, J.D. Wander, Oxidation chemistry of energetic materials in supercritical water, Hazard. Waste Hazard. Mater. 10 (1993) 233–246.

[36] D. Xu, S. Wang, X. Tang, Y. Gong, Y. Guo, Y. Wang, J. Zhang, Design of the first pilot scale plant of China for supercritical water oxidation of sewage sludge, Chem. Eng. Res. Des. 90 (2011) 288–297, http://dx.doi.org/10.1016/j.cherd.2011.06.013.

[37] V.G. Gude, Energy consumption and recovery in reverse osmosis, Desalin. Water Treat. 36 (2011) 239–260, http://dx.doi.org/10.5004/dwt.2011.2534.

[38] B. Peñate, L. García-Rodríguez, Current trends and future prospects in the design of seawater reverse osmosis desalination technology, Desalination 284 (2012) 1–8, http://dx.doi.org/10.1016/j.desal.2011.09.010.

[39] T. Davis, S. Rayman, Zero Discharge Seawater Desalination: Integrating the Production of Freshwater, Salt, Magnesium, and Bromine, (2006).

[40] UNESCO-WWAP, Water for People, Water for Life, (2003).

[41] Sigma-Aldrich, Safety Data Sheet, (2014).

[42] D.E. López, J.P. Trembly, Desalination of hypersaline brines with joule-heating and chemical pre-treatment: conceptual design and economics, Desalination 415 (2017)

49–57, http://dx.doi.org/10.1016/j.desal.2017.04.003.

[43] M.M. Dipippo, K. Sako, J.W. Tester, Ternary phase equilibria for the sodium chloride – sodium sulfate – water system at 200 and 250 bar up to 400 °C, Fluid Phase Equilib. 157 (1999) 229–255.

[44] F.J. Armellini, J.W. Tester, G.T. Hong, Precipitation of sodium chloride and sodium sulfate in water from sub- to supercritical conditions: 150 to 550 °C, 100 to 300 bar, J. Supercrit. Fluids 7 (1994) 147–158, http://dx.doi.org/10.1016/0896-8446(94)90019-1.

[45] P. Geisler, F.U. Hahnenstein, W. Krumm, T. Peters, Pressure exchange system for energy recovery in reverse osmosis plants, Desalination 122 (1999) 151–156, http://dx.doi.org/10.1016/S0011-9164(99)00036-3.

[46] G. Migliorini, E. Luzzo, Seawater reverse osmosis plant using the pressure exchanger for energy recovery: a calculation model, Desalination 165 (2004)

289–298, http://dx.doi.org/10.1016/j.desal.2004.06.034.

[47] V. Vadillo, J. Sanchez-Oneto, J.R. Portela, E.J.M. de la Ossa, Problems in supercritical water oxidation process and proposed solutions, Ind. Eng. Chem. Res. 52 (2013) 7617–7629, http://dx.doi.org/10.1021/ie400156c.

[48] I. Leusbrock, Removal of Inorganic Compounds Via Supercritical Water: Fundamentals and Applications, Rijksuniversiteit Groningen, 2011.

[49] W. Wagner, J.R. Cooper, A. Dittmann, J. Kijima, H.J. Kretzschmar, A. Kruse, R. Mares, K. Oguchi, H. Sato, I. Stocker, O. Sifner, Y. Takaishi, I. Tanishita, J. Trubenbach, T. Willkommen, The IAPWS industrial formulation 1997 for the thermodynamic properties of water and steam, J. Eng. Gas Turbines Power 122 (2000) 150–182.

[50] R. Sinnott, Coulson & Richardson's Chemical Engineering Series: Chemical Engineering Design, 5th ed., Elsevier Butterworth-Heinemann, Oxford, 2005.